

Spin dynamics of the triangular Heisenberg antiferromagnet: A Schwinger-boson approach

Ann Mattsson

*Institute of Theoretical Physics, Chalmers University of Technology and Göteborg University,
S-412 96 Göteborg, Sweden*

(Received 27 September 1994)

We have analyzed the two-dimensional antiferromagnetic Heisenberg model on the triangular lattice using a Schwinger-boson mean-field theory. By expanding around a state with local 120° order, we obtain, in the limit of infinite spin, results for the excitation spectrum in complete agreement with linear spin-wave theory (LSWT). In contrast to LSWT, however, the modes at the ordering wave vectors acquire a mass for finite spin. We discuss the origin of this effect.

INTRODUCTION

The two-dimensional spin- $\frac{1}{2}$ Heisenberg antiferromagnet (HAFM) has received much attention during the last few years. The main reason for this new interest stems from the discovery of the ceramic superconductors, which has led to extensive studies of the HAFM on a square lattice.¹ An important focal point has been the experimentally observed competition between superconductivity and antiferromagnetic order in these materials. This has encouraged numerous investigations of disordering effects, in particular the role of frustrating interactions.

To elucidate the role of frustration, it is interesting to study cases where frustration is intrinsic to the lattice structure such as the HAFM on a triangular or Kagomé lattice. Early papers on the triangular HAFM (Refs. 2 and 3) suggested that the spin- $\frac{1}{2}$ ground state is a spin liquid, lacking long-range order (LRO). More recent studies⁴⁻⁹ point to the scenario of an ordered ground state possibly quite close to a disordering transition. Yet other studies support the original proposal of a disordered ground state.^{10,11}

The spin dynamics of the model, intimately linked to the character of the ground state, also remains an open question. The problem of the spin dynamics above a ground state with Néel-type order (a 120° state) has been attacked with a variety of methods, like linear spin-wave theory (LSWT),⁵ nonlinear σ model,¹² and Schwinger-boson mean-field theory (SBMFT).^{6,13} The SBMFT has proved successful in incorporating quantum fluctuations,¹⁴ but the choice of mean-field parameters is a delicate matter.^{15,16} Yoshioka and Miyazaki⁶ have used the SBMFT combined with a resonant valence bond ansatz, and a similar theory including a ferromagnetic component in the mean-field expansion is recently analyzed by Lefmann and Hedegård.¹³ A drawback of these applications of SBMFT is that the LSWT structure of the dispersion relation cannot be recovered in the limit of infinite spin. Specifically, only two massless spin-wave modes can be obtained, in contrast to the three massless modes of LSWT. This is a weakness, since, at an analytical level, the only reliable way to motivate the va-

lidity of the theory is to use an approach that correctly reproduces the limit of classical magnetism.¹⁶

We here employ another mean-field treatment, where we use a spin rotation to identify the relevant mean-field parameters, treating the spin dynamics above a state close to the classical ground state. In this way *three* modes are obtained, two of which exhibit a massgap at finite spin. However, in the limit of infinite spin, the gap asymptotically vanishes on the relevant energy scale and the corresponding spin-wave velocities exactly approach those of LSWT. We discuss the origin of massgaps within this version of SBMFT and "explain" why there are no gaps in LSWT at any value of the spin.

THE MODEL

We consider the Hamiltonian

$$\mathcal{H} = J_1 \sum_{\mathbf{R}, \alpha} \mathbf{S}_{\mathbf{R}} \cdot \mathbf{S}_{\mathbf{R}+\alpha} , \quad (1)$$

defined on a triangular lattice and with $J_1 \geq 0$. The sums run over all lattice sites \mathbf{R} and three of the six nearest-neighbor vectors α . We choose the vectors α to be

$$\alpha_1 = -\frac{1}{2}\mathbf{e}_x - \frac{\sqrt{3}}{2}\mathbf{e}_y , \quad (2a)$$

$$\alpha_2 = -\frac{1}{2}\mathbf{e}_x + \frac{\sqrt{3}}{2}\mathbf{e}_y , \quad (2b)$$

$$\alpha_3 = \mathbf{e}_x , \quad (2c)$$

in units where the lattice constant equals 1 (see Fig. 1).

The triangular lattice is a Bravais lattice and can be divided into three equal interlacing sublattices (tripartite lattice). In Fig. 1 the three sublattices are indicated. It follows that in the classical limit of large spin, the ground state is a 120° state, i.e., a coplanar state with spins on each sublattice being ferromagnetically ordered and rotated 120° vis a vis the spins on the two other

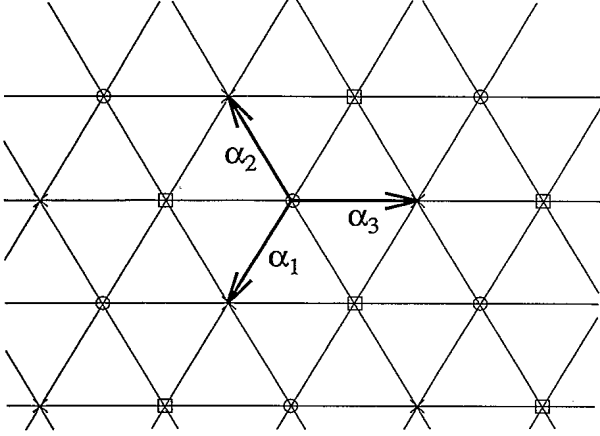


FIG. 1. Triangular lattice. The vectors α point to half the number of nearest neighbors of a site. Sites of the three sublattices are indicated by squares, crosses, and circles, respectively.

sublattices. (The lattice constant of a sublattice is $\sqrt{3}$ times the nearest-neighbor spacing, that is why this state also is called a “ $\sqrt{3} \times \sqrt{3}$ state.”)

When expanding around such a 120° state, it is convenient to start with a local rotation of the spin coordinate system. The spins on neighboring sublattices are rotated by $+120^\circ$ around the y axis when going from \mathbf{R} to $\mathbf{R} + \alpha$ (to go in the $+\alpha$ and in the $-\alpha$ directions is not equivalent since the 120° state breaks parity, note that in two dimensions a parity transformation is defined by a reflection in a line):

$$S_{\mathbf{R}}^x \rightarrow \cos(\mathbf{Q} \cdot \mathbf{R}) S_{\mathbf{R}}^x + \sin(\mathbf{Q} \cdot \mathbf{R}) S_{\mathbf{R}}^z, \quad (3a)$$

$$S_{\mathbf{R}}^y \rightarrow S_{\mathbf{R}}^y, \quad (3b)$$

$$S_{\mathbf{R}}^z \rightarrow \cos(\mathbf{Q} \cdot \mathbf{R}) S_{\mathbf{R}}^z - \sin(\mathbf{Q} \cdot \mathbf{R}) S_{\mathbf{R}}^x, \quad (3c)$$

where \mathbf{Q} is defined by $\mathbf{Q} \cdot \alpha = \frac{2\pi}{3} + 2\pi n$ with n integer. This implies that

$$\begin{aligned} \mathbf{S}_{\mathbf{R}} \cdot \mathbf{S}_{\mathbf{R}+\alpha} &\rightarrow \frac{\sqrt{3}}{2} (S_{\mathbf{R}}^z S_{\mathbf{R}+\alpha}^x - S_{\mathbf{R}}^x S_{\mathbf{R}+\alpha}^z) \\ &\quad - \frac{1}{2} (S_{\mathbf{R}}^z S_{\mathbf{R}+\alpha}^z + S_{\mathbf{R}}^x S_{\mathbf{R}+\alpha}^x) + S_{\mathbf{R}}^y S_{\mathbf{R}+\alpha}^y. \end{aligned} \quad (4)$$

Let us pick a specific 120° state, with the (unrotated) spins on the first sublattice pointing in the z direction while on the other two sublattices they span the x - z plane with directions -120° ($+120^\circ$) with respect to the z axis when going in the α ($-\alpha$) direction in the lattice. Any classical ground state can clearly be reached from this state by a (global) $\text{SO}(3)$ rotation of the spins. We immediately see that the spin rotation in Eqs. (3) transfers this 120° state into a ferromagnetic state with quantization axes lying in the x - z plane. The first term in Eq. (4) vanishes when acting on a ferromagnetic state, and we may hence neglect it when modeling states with a local structure close to a 120° state. In the rotated basis, the effective Hamiltonian is thus given by

$$\mathcal{H} = J_1 \sum_{\mathbf{R}, \alpha} -\frac{1}{2} (S_{\mathbf{R}}^x S_{\mathbf{R}+\alpha}^x + S_{\mathbf{R}}^z S_{\mathbf{R}+\alpha}^z) + S_{\mathbf{R}}^y S_{\mathbf{R}+\alpha}^y. \quad (5)$$

We have verified that in our case this approach is equivalent to that in Ref. 17 where an analysis of the frustrated model on the square lattice is performed. It is interesting to note that in LSWT the term that corresponds to $\frac{\sqrt{3}}{2} (S_{\mathbf{R}}^z S_{\mathbf{R}+\alpha}^x - S_{\mathbf{R}}^x S_{\mathbf{R}+\alpha}^z)$ in Eq. (4) is also neglected since it is cubic in the Holstein-Primakoff bosons.

The Schwinger-boson calculation that follows is similar to the treatment of the $J_1 - J_2$ model on the square lattice¹⁸ and on the honeycomb lattice.¹⁹ The spin operators $\mathbf{S}_{\mathbf{R}}$ at each lattice site are replaced by two species of Schwinger bosons $b_{\mu\mathbf{R}}^\dagger$ ($\mu = 1, 2$) via

$$\mathbf{S}_{\mathbf{R}} = \frac{1}{2} b_{\mu\mathbf{R}}^\dagger \boldsymbol{\sigma}_{\mu\nu} b_{\nu\mathbf{R}}, \quad (6)$$

with the local constraints $b_{\mu\mathbf{R}}^\dagger b_{\mu\mathbf{R}} = 2S$. Here $\boldsymbol{\sigma} = (\sigma^x, \sigma^y, \sigma^z)$ is the vector of Pauli matrices, and summation over repeated (Greek) indices is implied. This leads us to the following Hamiltonian:

$$\begin{aligned} \mathcal{H} = &-J_1 \sum_{\mathbf{R}, \alpha} \left(-\frac{3}{4} \mathcal{W}_{\mathbf{R}, \alpha}^A + \frac{1}{4} \mathcal{W}_{\mathbf{R}, \alpha}^B \right) \\ &+ \sum_{\mathbf{R}} \lambda_{\mathbf{R}} [b_{\mu\mathbf{R}}^\dagger b_{\mu\mathbf{R}} - 2S], \end{aligned} \quad (7)$$

where we have included the local constraints with Lagrange multipliers $\lambda_{\mathbf{R}}$ at each site. The expression for the summands is

$$\mathcal{W}_{\mathbf{R}, \alpha}^X = \frac{1}{2} : \mathcal{X}_{\mathbf{R}, \alpha}^\dagger \mathcal{X}_{\mathbf{R}, \alpha} : - S^2, \quad (8)$$

with $\mathcal{X}_{\mathbf{R}, \alpha}$ any of the two link operators

$$\mathcal{A}_{\mathbf{R}, \alpha} \equiv b_{1\mathbf{R}} b_{1\mathbf{R}+\alpha} + b_{2\mathbf{R}} b_{2\mathbf{R}+\alpha}, \quad (9a)$$

$$\mathcal{B}_{\mathbf{R}, \alpha} \equiv b_{1\mathbf{R}}^\dagger b_{1\mathbf{R}+\alpha} + b_{2\mathbf{R}}^\dagger b_{2\mathbf{R}+\alpha}. \quad (9b)$$

The mean-field theory is finally generated by the Hartree-Fock decoupling

$$\begin{aligned} : \mathcal{X}_{\mathbf{R}, \alpha}^\dagger \mathcal{X}_{\mathbf{R}, \alpha} : &\rightarrow \mathcal{X}_{\mathbf{R}, \alpha}^\dagger \langle \mathcal{X}_{\mathbf{R}, \alpha} \rangle + \langle \mathcal{X}_{\mathbf{R}, \alpha}^\dagger \rangle \mathcal{X}_{\mathbf{R}, \alpha} \\ &\quad - \langle \mathcal{X}_{\mathbf{R}, \alpha}^\dagger \rangle \langle \mathcal{X}_{\mathbf{R}, \alpha} \rangle, \end{aligned} \quad (10)$$

where the link fields (mean-field parameters) $Q_1 \equiv \langle \mathcal{A}_{\mathbf{R}, \alpha} \rangle$ and $Q_2 \equiv \langle \mathcal{B}_{\mathbf{R}, \alpha} \rangle$ are taken to be uniform and real. In our mean-field treatment, we also replace the local Lagrange multipliers $\lambda_{\mathbf{R}}$ by a single parameter λ .

For comparison of our results with those of LSWT (Ref. 5) it is convenient to Fourier-transform the Schwinger bosons independently on each sublattice:

$$b_{\mu\mathbf{R}_m} = \frac{1}{\sqrt{N/2}} \sum_{\mathbf{k}} e^{-i\mathbf{k} \cdot \mathbf{R}_m} a_{m\mu\mathbf{k}}, \quad m = 1, 2, 3, \quad (11)$$

with \mathbf{R}_1 , \mathbf{R}_2 , and \mathbf{R}_3 on the three different sublattices, respectively. We then need to decouple the different bosons on the sublattices. This is done by the canonical transformations

$$a_{1\mu k} = \frac{1}{\sqrt{3}} (\beta_{1\mu k} + \beta_{2\mu k} + \beta_{3\mu k}), \quad (12a)$$

$$a_{2\mu k} = \frac{1}{\sqrt{3}} (\beta_{1\mu k} + j^* \beta_{2\mu k} + j \beta_{3\mu k}), \quad (12b)$$

$$a_{3\mu k} = \frac{1}{\sqrt{3}} (\beta_{1\mu k} + j \beta_{2\mu k} + j^* \beta_{3\mu k}), \quad (12c)$$

where $j = \exp(i\frac{2\pi}{3})$.

Finally we use the Bogoliubov transformations

$$\beta_{1\mu k} = \cosh \vartheta_{1k} c_{1\mu k} + \sinh \vartheta_{1k} c_{1\mu-k}^\dagger, \quad (13a)$$

$$\beta_{2\mu k} = \cosh \vartheta_{2k} c_{2\mu k} + \sinh \vartheta_{2k} c_{3\mu-k}^\dagger, \quad (13b)$$

$$\beta_{3\mu k} = \cosh \vartheta_{3k} c_{3\mu k} + \sinh \vartheta_{3k} c_{2\mu-k}^\dagger, \quad (13c)$$

with

$$\tanh(2\vartheta_{mk}) = \frac{\frac{9}{2} J_1 Q_1 \gamma_{m,k}}{\lambda + \frac{3}{2} J_1 Q_2 \gamma_{m,k}}, \quad m = 1, 2, 3, \quad (14)$$

to diagonalize the resulting Hamiltonian. This yields free bosons $c_{m\mu k}$ with dispersion relations

$$\omega_{mk} = \sqrt{(\lambda + \frac{3}{2} J_1 Q_2 \gamma_{m,k})^2 - (\frac{9}{2} J_1 Q_1 \gamma_{m,k})^2}, \quad m = 1, 2, 3, \quad (15)$$

where the geometrical factors are given by

$$\gamma_{1,k} = \frac{1}{6} \sum_{\alpha} \cos(\mathbf{k} \cdot \boldsymbol{\alpha}), \quad (16a)$$

$$\gamma_{2,k} = \frac{1}{6} \sum_{\alpha} \cos\left(\mathbf{k} \cdot \boldsymbol{\alpha} + \frac{2\pi}{3}\right), \quad (16b)$$

$$\gamma_{3,k} = \frac{1}{6} \sum_{\alpha} \cos\left(\mathbf{k} \cdot \boldsymbol{\alpha} - \frac{2\pi}{3}\right). \quad (16c)$$

By minimizing the free energy we obtain the three equations needed to determine the mean-field parameters:

$$\frac{1}{3} \sum_{m=1}^3 \int \frac{d^2 k}{A} \cosh(2\vartheta_{mk}) (n_{mk} + \frac{1}{2}) - (S + \frac{1}{2}) = 0, \quad (17a)$$

$$\frac{1}{3} \sum_{m=1}^3 \int \frac{d^2 k}{A} \sinh(2\vartheta_{mk}) \gamma_{m,k} (n_{mk} + \frac{1}{2}) - \frac{1}{2} Q_1 = 0, \quad (17b)$$

$$\frac{1}{3} \sum_{m=1}^3 \int \frac{d^2 k}{A} \cosh(2\vartheta_{mk}) \gamma_{m,k} (n_{mk} + \frac{1}{2}) - \frac{1}{2} Q_2 = 0. \quad (17c)$$

Here $A = 8\pi^2/(3\sqrt{3})$ is the area of the reciprocal unit cell of a sublattice, and $n_{mk} = [\exp(\beta\omega_{mk}) - 1]^{-1}$ is the Bose occupation number. Solving the mean-field equations numerically yields values for Q_1 , Q_2 , and λ , which are used to determine thermodynamic quantities at finite

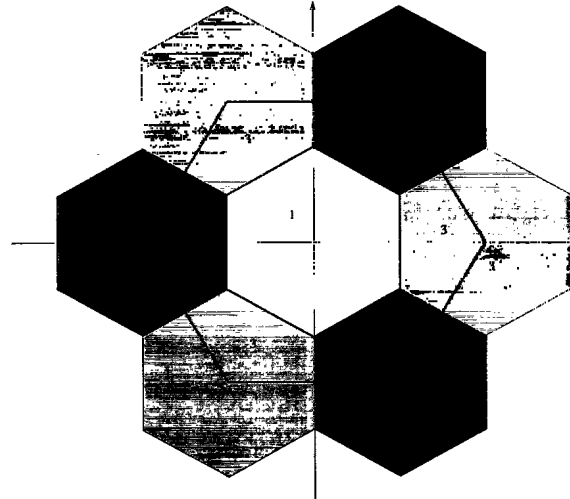


FIG. 2. The Brillouin zones of the triangular lattice (large) and of the sublattices (small). The numbers 1 to 3 are indicating the parts of the large Brillouin zone that corresponds to the three different modes in the small Brillouin zone. Three possible vectors \mathbf{Q} (see text) are also shown.

temperatures.

Given a Bravais lattice, as in the present case, a division into sublattices is not necessary when Fourier-transforming (as it is on a non-Bravais lattice) and the theory may be formulated in terms of only one set of bosons. We have chosen to transform each sublattice independently in order to make the comparison with LSWT results more transparent. In our treatment we thus have a small Brillouin zone and three sets of bosons (picture A), which is equivalent to picture B where the larger Brillouin zone of the real lattice and one of the sets of bosons (say $c_{1\mu k}$) is used (see Fig. 2). The equivalence of the two pictures makes it evident why $c_{2\mu k}$ has to be combined with $c_{3\mu-k}$ in Eqs. (13b) and (13c). It also explains the structure of the geometrical factors in Eq. (16) (remembering that $\mathbf{Q} \cdot \boldsymbol{\alpha} = \frac{2\pi}{3}$). Until now we have used picture A, but, e.g., in the figures we will use picture B (one mode) instead of showing plots for three different modes. Since modes 2 and 3 in picture A are degenerate we will sometimes refer to them as the corner modes which is picture B language. To avoid confusion we indicate in the following which picture we use.

ZERO-TEMPERATURE FORMALISM

In two dimensions there can be LRO only at zero temperature. This means that exactly at $T = 0$ there is an abrupt phase transition, and we must be careful when reducing T to zero. As we see from Eq. (17), the parameters Q_1 , Q_2 , and λ will depend on temperature via the Bose occupation number n_{mk} , and hence, to calculate properties at $T = 0$ we need to pass to a zero-temperature formalism. Following Ref. 20 we note that LRO corresponds to a condensation of the Schwinger bosons at some points \mathbf{K}_m in the Brillouin zone and we obtain the mean-field equations at $T = 0$ from Eq. (17) by the replacement

$$\frac{n_{mk}}{\omega_{mk}} \rightarrow S_m^* \delta^{(2)}(\mathbf{k} - \mathbf{K}_m) , \quad (18)$$

where S_m^* is a new unknown quantity measuring the Bose condensate. Since the condensation of the bosons implies that there is no gap in the spin-wave spectrum [$\omega_{m\mathbf{k}=\mathbf{K}_m} = 0$ in (15)] at $T = 0$, these m equations together with the three equations in (17) are sufficient to determine the $3 + m$ parameters λ , Q_1 , Q_2 , and S_m^* . The procedure is the following: We start at a finite temperature and use Eqs. (17) to determine the mean-field parameters which gives us the dispersion relation. We then lower the temperature and examine the dispersion relation to identify the points in the Brillouin zone where the gap scales down with temperature. In our case this happens for each of the three modes (picture A) at $\mathbf{k} = \mathbf{0}$. We expand the dispersion relation around these points and for small \mathbf{k} the dispersion relations (15) takes the relativistic form $\omega_{m\mathbf{k}} = c_m \sqrt{(M_m c_m)^2 + |\mathbf{k}|^2}$. Carrying out the expansion we find that the spin-wave velocities c_m are given by

$$c_1 = \sqrt{\left(\frac{9}{4}J_1Q_1\right)^2 \frac{1}{2} - \frac{3}{8}J_1Q_2\left(\lambda + \frac{3}{4}J_1Q_2\right)} \quad (19)$$

and

$$c_2 = c_3 = \sqrt{\left(\frac{9}{8}J_1Q_1\right)^2 \frac{1}{2} + \frac{3}{16}J_1Q_2\left(\lambda - \frac{3}{8}J_1Q_2\right)} . \quad (20)$$

The masses M_m in the energy gap $\Delta_m = M_m c_m^2$ of the spin-wave excitations can in turn be extracted from

$$\Delta_1 = \sqrt{\left(\lambda + \frac{3}{4}J_1Q_2\right)^2 - \left(\frac{9}{4}J_1Q_1\right)^2} \quad (21)$$

and

$$\frac{\omega_{m\mathbf{k}}}{J_1} = \sqrt{\left[\frac{\lambda}{J_1} + \frac{3}{2}(3Q_1 + Q_2)\gamma_{m,\mathbf{k}}\right]\left[\frac{\lambda}{J_1} - \frac{3}{2}(3Q_1 - Q_2)\gamma_{m,\mathbf{k}}\right]} , \quad (23)$$

which immediately can be compared with the LSWT result, Eq. (13) in Ref. 5. To get the LSWT results we need $Q_1 = Q_2 = \frac{2}{3}\frac{\lambda}{J_1}$, which is (as we have already seen) the condition to obtain three massless modes ($\Delta_1 = \Delta_2 = \Delta_3 = 0$). Thus, in the limit of infinitely large spin, where we in fact obtain three massless modes,

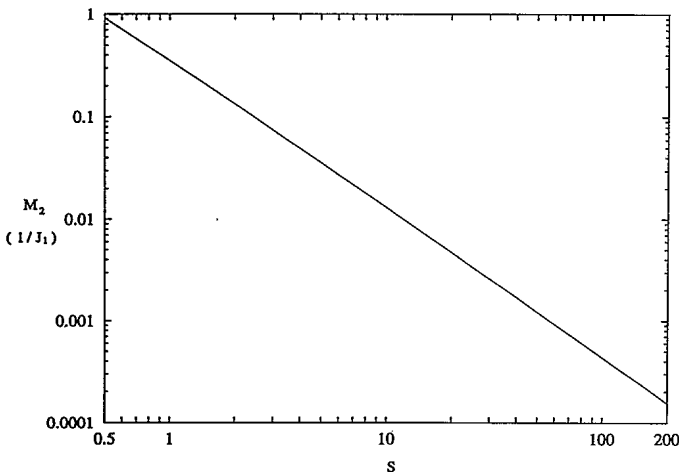


FIG. 3. The mass $M_2 (= M_3)$ of the corner modes [picture B (see text)] vs spin S .

$$\Delta_2 = \Delta_3 = \sqrt{\left(\lambda - \frac{3}{8}J_1Q_2\right)^2 - \left(\frac{9}{8}J_1Q_1\right)^2} . \quad (22)$$

To examine whether we have condensation of bosons for all modes, we first consider the gaps, or the masses, since condensation of the bosons at $\mathbf{K}_m = \mathbf{0}$ implies that we have no gap in the spectrum at this point. To get all modes massless ($\Delta_1 = \Delta_2 = \Delta_3 = 0$) we need to have $Q_1 = Q_2 = \frac{2}{3}\frac{\lambda}{J_1}$ [from Eqs. (21) and (22)]. Since $\gamma_{1,0} = \frac{1}{2}$ and $\gamma_{2,0} = \gamma_{3,0} = -\frac{1}{4}$ we see from Eq. (14) that we must have equalities between *finite* quantities as $\omega_{10} \sinh(2\vartheta_{10}) = \omega_{10} \cosh(2\vartheta_{10})$ and $\omega_{20} \sinh(2\vartheta_{20}) = \omega_{30} \sinh(2\vartheta_{30}) = -\omega_{20} \cosh(2\vartheta_{20}) = -\omega_{30} \cosh(2\vartheta_{30})$. But doing the replacement in Eq. (18) into Eq. (17) for all three modes then gives $Q_1 \neq Q_2$ from Eqs. (17b) and (17c), in contradiction to the initial assumption. The only way to get three massless modes is to have $\omega_{10} \sinh(2\vartheta_{10}) = \omega_{10} \cosh(2\vartheta_{10})$ *infinite*, which then yields $Q_1 = Q_2$ at *infinite spin S* as seen from Eq. (17a).

The result of the procedure above is that for finite spin S we will get a condensation of the bosons only for the first mode which scales faster to zero than the two other modes. For this mode we do the replacement shown in Eq. (18) ($m = 1$ and $\mathbf{K}_1 = \mathbf{0}$) into Eq. (17) ($S_2^* = S_3^* = 0$) and since $\Delta_1 = 0$, Eq. (21) gives λ in terms of Q_1 and Q_2 . After these substitutions we have no temperature dependence in Eqs. (17).

With this zero-temperature formalism we have studied the *spin* dependence of the mass $M_2 (= M_3)$. As we see in Fig. 3 the mass goes to zero in the limit of infinitely large spin and we recover the three massless modes of LSWT. The dispersion relation in Eq. (15) can be rewritten as

we *exactly* recover the LSWT results. In Fig. 4 we show the dispersion relation for two values of the spin S . We see that on the relevant energy scale the gaps at the corners (picture B) go to zero and for infinite spin we recover the LSWT dispersion relation.

We have also calculated the spin-wave velocities c_m ($m = 1, 2, 3$) at $T = 0$. In Fig. 5 we see the results compared with the LSWT results extracted from Ref. 5 (which agree with the nonlinear σ model results in Ref. 12): $c_1^{\text{LSWT}} = \frac{3\sqrt{3}}{2}J_1S$ and $c_2^{\text{LSWT}} = c_3^{\text{LSWT}} = c_1^{\text{LSWT}}/\sqrt{2}$. For large spin S we have good agreement with these results. We have also examined the ratio of the two spin-wave velocities, as shown in Fig. 6.

DISCUSSION

To summarize, we have performed a SBMFT analysis of the spin dynamics of the antiferromagnetic Heisenberg model on a triangular lattice, expanding around a state with local 120° order. Considering that the 120° state has been favored as a candidate ground state in several studies, this is a natural approach. In order to identify the relevant fields in such an expansion, we have performed a spin rotation and we have also neglected the

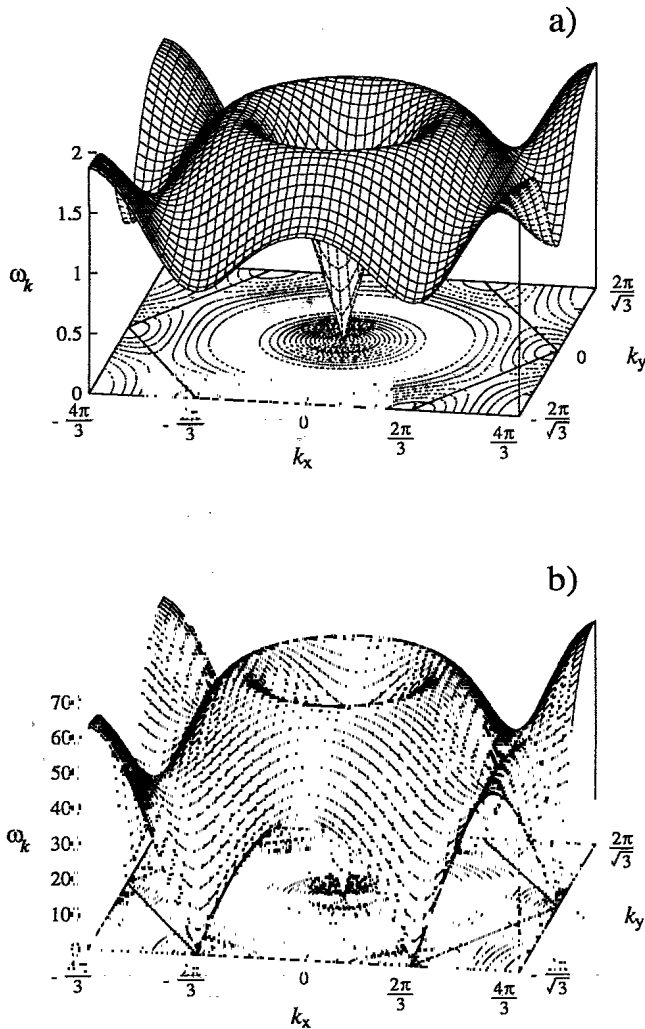


FIG. 4. The dispersion relation for spin (a) $S = 0.5$ and (b) $S = 200$ at zero temperature. The gap at the “ferromagnetic” point is always zero while the gap at the “antiferromagnetic” points only tends to zero for large spin. We use picture B (see text).

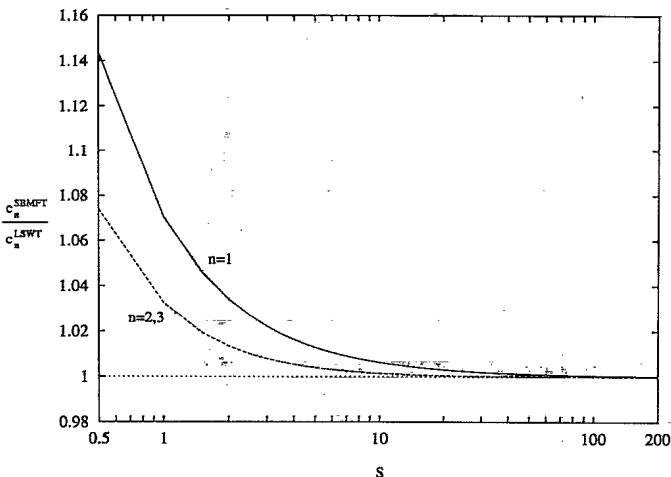


FIG. 5. The ratio of the spin-wave velocities c_m , $m = 1, 2, 3$, obtained by our theory (SBMFT) and by LSWT (or by Ref. 12) vs spin S .

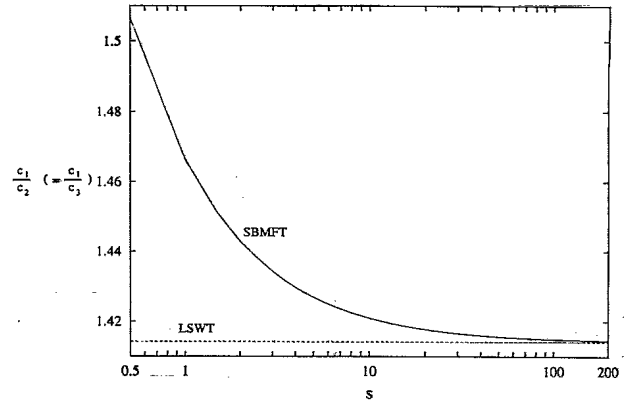


FIG. 6. The ratio between the center mode spin-wave velocity c_1 and the corner mode [picture B (see text)] spin-wave velocities $c_2 (= c_3)$ vs spin S compared with the LSWT result $\sqrt{2}$.

part of the Hamiltonian which gives no contribution in the classical limit.

In the limit of infinitely large spin we obtain three massless modes in the dispersion relation of the spin waves, exactly recovering the LSWT results, including the spin-wave velocities. This is an improvement on earlier SBMFT calculations on the triangular lattice,^{6,13} where the $S \rightarrow \infty$ limit does not come out correctly. At finite spin, however, two of the modes acquire a mass. This can be understood as follows: The effective Hamiltonian in Eq. (5) is invariant under rotations in the x - z plane, and the $SU(2)$ symmetry of the original model is lowered to $U(1)$. Since the 120° state breaks this $U(1)$ symmetry, we should obtain *one* Goldstone mode, which agrees with our results for finite spin. We do not believe that the massiveness of the other modes are due to enhanced quantum fluctuations at finite spin: If the effective Hamiltonian had preserved the $SU(2)$ symmetry of the full Hamiltonian we should probably have recovered the three Goldstone modes as expected. We are also led to this conclusion by the discussion in Ref. 16 where the analogous problem of the frustrated square lattice model is considered.

We have already mentioned that the term in the full Hamiltonian that we neglect in order to obtain the effective Hamiltonian is also neglected in LSWT. Yet, LSWT predicts three massless modes for arbitrary spin, even though the LSWT Hamiltonian is not $SU(2)$ invariant. From Fig. 3 we see that for large spin the mass $M_2 (= M_3)$ goes approximately as $S^{-1.5}$ and from Fig. 5 we see that the spin-wave velocities goes like the LSWT result, that is, they are proportional to S . Thus, the energy gap goes like $S^{-1.5} * S^2 = S^{0.5}$. Since the energy in LSWT only retains powers of S larger than or equal to 1 and the massgap is approximately proportional to $S^{0.5}$, one still obtains massless modes in LSWT. In the same sense that LSWT is correct for large spin (neglecting terms of order S^n , $n < 1$) our results are valid for large spins, neglecting energy terms of the order of the massgap.

It is interesting to note that the modes at the corners of the Brillouin zone (picture *B*) describes fluctuations in the y component of the spin, while the center mode describes in-plane fluctuations.¹² The first term in Eq. (4) is independent of the y component, which means that fluctuations in this component are described equally well by the effective and the full Hamiltonian. This makes the value of the spin-wave velocity at the corner modes more reliable than that at the center mode, since this last value directly depends on the difference between the effective and the full Hamiltonian.

It should be interesting to perform an extended analysis of the spin dynamics above a state with local 120° order. Starting with the approach of Lefmann and Hedegård,¹³ one may write the Hamiltonian in terms of a singlet field (also considered by Yoshioka and Miyazaki⁶) and a field representing the ferromagnetic correlations,

and then perform a spin rotation. Certain pieces of the two fields then combine to a constant term and the remaining parts can be written in terms of four effective fields. Diagonalizing this form of the Hamiltonian using the SBMFT may possibly yield a dispersion relation which can take all solutions into account *within the same mean-field theory*. The solution presented in this paper is valid for large spin, as we have already argued, but this approach may help answering for which magnitudes of the spin the solutions of Refs. 6 and 13 are relevant. We will return to this subject.

ACKNOWLEDGMENTS

We thank H. Johannesson, P. Fröjdh, and A. Chubukov for discussions and valuable remarks.

¹ For a review of the unfrustrated spin- $\frac{1}{2}$ square Heisenberg antiferromagnet, see E. Manousakis, *Rev. Mod. Phys.* **63**, 1 (1991).

² P. W. Anderson, *Mater. Res. Bull.* **8**, 153 (1973).

³ V. Kalmeyer and R. B. Laughlin, *Phys. Rev. Lett.* **59**, 2095 (1987).

⁴ David A. Huse and Veit Elser, *Phys. Rev. Lett.* **60**, 2531 (1988).

⁵ Th. Jolicoeur and J. C. Le Guillou, *Phys. Rev. B* **40**, 2727 (1989).

⁶ D. Yoshioka and J. Miyazaki, *J. Phys. Soc. Jpn.* **60**, 614 (1991).

⁷ Rajiv R. P. Singh and David A. Huse, *Phys. Rev. Lett.* **68**, 1766 (1992).

⁸ B. Bernu, C. Lhuillier, and L. Pierre, *Phys. Rev. Lett.* **69**, 2590 (1992).

⁹ N. Elstner, R. R. P. Singh, and A. P. Young, *Phys. Rev. Lett.* **71**, 1629 (1993).

¹⁰ Y. R. Wang, *Phys. Rev. B* **45**, 12 604 (1992).

¹¹ Kun Yang, L. K. Warman, and S. M. Girvin, *Phys. Rev. Lett.* **70**, 2641 (1993).

¹² T. Dombre and N. Read, *Phys. Rev. B* **39**, 6797 (1989).

¹³ Kim Lefmann and Per Hedegård, *Phys. Rev. B* **50**, 1074 (1994).

¹⁴ D. P. Arovas and A. Auerbach, *Phys. Rev. B* **38**, 316 (1988); A. Auerbach and D. P. Arovas, *Phys. Rev. Lett.* **61**, 617 (1988).

¹⁵ H. A. Ceccatto, C. J. Gazza, and A. E. Trumper, *Phys. Rev. Lett.* **72**, 1943 (1994).

¹⁶ P. Coleman and P. Chandra, *Phys. Rev. Lett.* **72**, 1944 (1994).

¹⁷ P. Chandra, P. Coleman, and A. I. Larkin, *J. Phys. Condens. Matter* **2**, 7933 (1990).

¹⁸ T. Einarsson, P. Fröjdh, and H. Johannesson, *Phys. Rev. B* **45**, 13 121 (1992).

¹⁹ Ann Mattsson, P. Fröjdh, and T. Einarsson, *Phys. Rev. B* **49**, 3997 (1994).

²⁰ M. Takahashi, *Phys. Rev. B* **40**, 2494 (1989).